Multiple Electron Scattering through a Slab*

J. H. Jacob
AVCO Everett Research Laboratory, a Division of AVCO Corporation, Everett, Massachusetts 02149
(Received 7 December 1972)

The transport equation for electron scattering through plane parallel targets has been solved by expanding the electron distribution function into spherical harmonics. The electron energy is assumed to be constant. No simplifying assumptions have been made concerning the scattering cross sections. In fact, a simple technique has been found for accurately determining the screening angle which plays an important role in multiple scattering. For small angles ($\leq 10°$) and thin targets, the emerging electron distribution agrees well with earlier theories. However, for larger angles the present theory predicts a greater probability of scattering than earlier theories. For thin targets it is well known that the earlier theories merge with the single-scattering distribution function at large angles. This difference at large angles between the present and earlier theories implies that the electron distribution predicted by the present calculations will not merge with the single-scattering distribution. For thick targets, as one would expect, the earlier theories are poor approximations of the emergent electron distribution function for all angles.

I. INTRODUCTION

Multiple electron scattering has been a topic of interest for the last half-century. In the first treatment of electron scattering through thin foils the emerging distribution function of electrons was broken into two regions: For small angles it was assumed that the electron had suffered many collisions, whereas for large angles the emerging electron suffered only one collision. Hence for small angles one could calculate the mean square deflection per collision and then use a statistical theory which gives a Gaussian distribution. This Gaussian distribution was connected to the single-scattering tail.[1] Goudsmit and Saunderson[2] derived the angular distribution function in terms of Legendre polynomials. They also obtained a Gaussian at small angles that merged into the single-scattering tail at large angles. However, their theory has two major drawbacks: (a) it was assumed that all electrons "saw" the same target thickness, and (b) the boundary conditions were not included. Goudsmit and Saunderson argue that the difference in the path lengths can be accounted for by replacing the target thickness by $t/\langle\cos\theta\rangle_{av}$, where t is the thickness and θ is the angular deflection. Molière[3] subsequently indicated the fallacy of such an argument and pointed out that as a result of such an assumption Goudsmit and Saunderson's and other earlier theories were limited to small angles. Bethe[4] shows formally the connection between Molière's and Goudsmit and Saunderson's theories.

Wang and Guth[5] have studied the problem in considerable detail. They have compared and discussed different approximate methods of obtaining a solution. In fact, they derive the distribution function of electrons after penetrating a foil of given thickness. Their solution includes the exact boundary conditions. However, they found their result too complex for evaluation. Instead they revert to a perturbation technique that uses the Goudsmit-Saunderson result as the zeroth-order distribution. It is questionable whether such a scheme is valid, because at large angles the correction to the Goudsmit-Saunderson result is not small. For example, it is found that the exact distribution is almost a factor of 2 larger than Goudsmit and Saunderson's result.

Breitenberger[6] has also solved the problem of electron transport through a slab without the simplifying assumption that all electrons suffer the same number of collisions. For angles of 10° and less his complicated integral equation reduces to Goudsmit and Saunderson's formula.

In this paper the transport equation for electron scattering through a plane parallel target has been solved by expanding the electron distribution function into spherical harmonics. The solution is exact provided the electron energy is constant. The spherical harmonic expansion method has been applied to transport problems for over 30 years.[5] In the early forties this method was refined for problems of neutron transport.[7,8] However, the scattering cross section for neutrons is assumed to be nearly isotropic, whereas the electron scattering cross section is strongly anisotropic. The exact boundary conditions will be included in a manner similar to that of Bethe, Rose, and Smith.[9] However, we will not limit ourselves to small angles only.

Removal of the limitation of small angles is possible largely because Spencer[10] has shown that the Boltzmann collision integral may be computed analytically for most cross sections of interest. Even if this simplification were not known, a solu-

tion to the problem is possible; however, the computation would be cumbersome.

In Sec. II the transport equation is expanded in spherical harmonics. Section III discusses the scattering cross section; a simple curve-fitting technique is used to accurately estimate the screening angle η, which is of primary importance in multiple scattering. In Sec. V the emergent electron distribution function is evaluated for special cases and a comparison is made with Goudsmit and Saunderson's theory. It is found that for thin targets and small angles the present distribution function is in agreement with the earlier theories. However, for angles larger than about 10° the present theory predicts a larger probability of scattering. In fact, at angles of 60° there is a difference of a factor of 2 for the thinnest targets considered. The earlier theories of multiple scattering emerge with the single-scattering tail at these large angles, for the thin targets considered. The above difference between the present and earlier theories implies, contrary to what is generally believed, that the emergent electron distribution will not go into the single-scattering results, provided the transport equation applies. The Boltzmann equation is clearly not applicable for monolayer targets. For thin targets a more accurate solution than the Goudsmit-Saunderson distribution function is just the Goudsmit-Saunderson result divided by $\cos\theta$. Physically this correction comes about because the transport equation without energy loss conserves current. The approximate equation solved by Goudsmit and Saunderson violates current conservation. For thick targets the earlier theories differ from the present case for all angles, and it is unlikely that there is a simple correction connecting earlier theories with the present one.

These results are also compared with the experiment of Hanson, Lanzl, Lyman, and Scott.[11] A similar comparison was made previously by Spencer and Blanchard.[12] They used the Goudsmit and Saunderson distribution function and found discrepancies, too large to be explained by experimental errors, for angles larger than 10°. Finally, in Sec. VI the spatial variation of the electron number density in the foil is evaluated and discussed.

II. TRANSPORT EQUATION

The basic equation for multiple electron scattering, neglecting energy loss, is given by

$$\hat{u}\cdot\nabla f = N\int [f(\vec{r},\hat{u}') - f(\vec{r},\hat{u})]\sigma(|\hat{u}-\hat{u}'|)d\hat{u}', \qquad (1)$$

where f is the electron distribution function, $\hat{u}$ is the unit vector in the direction of the electron's motion, N is the number density of scatterers, and σ is the scattering cross section per unit solid angle.

For a uniform beam of electrons in the x and y directions, striking a plane parallel plate that has a thickness t in the z direction, Eq. (1) simplifies to

$$\mu\frac{\partial f}{\partial z} = N\int [f(z,\hat{u}') - f(z,\mu)]\sigma(\mu_0)d\hat{u}', \qquad (2)$$

where μ is the cosine of the angle between the electron trajectory and the z axis and μ_0 is the cosine of the angle between the incident and scattered electron trajectories.

Expanding the distribution function and the scattering cross section as a sum of Legendre polynomials

$$f = \sum_l A_l P_l(\mu), \qquad (3)$$

$$\sigma = \sum_l \sigma_l P_l(\mu_0). \qquad (4)$$

Substituting expansions (3) and (4) into Eq. (2) and making use of both the orthogonality relation and addition theorem for Legendre polynomials, Eq. (2) reduces to

$$\left(\frac{l}{2l-1}\right)\frac{\partial A_{l-1}}{\partial z} + \frac{l+1}{2l+3}\frac{\partial A_{l+1}}{\partial z} + 2\pi N A_l\int_{-1}^{+1} d\mu\,\sigma(\mu)[1-P_l(\mu)] = 0. \qquad (5)$$

III. SCATTERING CROSS SECTION

The scattering cross section is the screened Rutherford that is modified to include relativistic effects and inelastic scattering by orbital electrons. Spencer[10] has shown that for low-atomic-number materials, i.e., $Z<27$, the cross section may be written

$$\sigma(\theta) = \frac{Z^2e^4}{p^2v^4}\left(\frac{Z+1}{Z}\right)\left((1+2\eta-\cos\theta)^{-2} + \frac{\pi\alpha\beta}{\sqrt{2}}(1-\cos\theta)^{-3/2} - \tfrac{1}{2}(\beta^2+\pi\alpha\beta)(1-\cos\theta)^{-1}\right), \qquad (6)$$

where e is the electronic charge, $\alpha = Z/137$, v is the electron velocity, c is the velocity of light, $\beta = v/c$, and p is the momentum of the electron.

η accounts for the screening of the nucleus by orbital electrons, while the factor $(Z+1)/Z$ accounts for inelastic deflections.[4] The last two terms are the result of relativistic effects and they are obtained from the McKinley-Feshbach expansion of the complete Mott formulas.

It turns out that the relativistic effects are important at large angles and that for small angles, the choice of the screening parameter is important. Molière[3] derived the following expression for η using the Thomas-Fermi atomic model:

$$2\eta = (1.13 + 3.76\,\alpha^2/\beta^2)\chi_0^2, \tag{7}$$

where

$$\chi_0 = (\hbar/p)Z^{1/3}/0.885a_0$$

and a_0 is the Bohr radius.

Nigam, Sundaresan, and Ta-You Wu[13] have pointed out errors in Molière's calculations; they use, instead, the Dalitz screening angle given by

$$2\eta = \chi_0'^2\left[1 + 4\alpha\chi_0'\left(\frac{1-\beta^2}{\beta}\ln\chi_0' + \frac{0.231}{\beta} + 1.448\beta\right)\right], \tag{8}$$

where

$$\chi_0' = (\hbar/p)\mu Z^{1/3}/0.885a_0 .$$

For the Thomas-Fermi atom, $\mu = 1.12$.

For small angles the Thomas-Fermi model is not as accurate as the Hartree representation.[14] Center[15] has used a combination of the Hartree representation for small angles and the Thomas-Fermi representation for larger angles. Figure 1 shows various plots of $\sigma(\theta)$ vs θ. There is considerable difference between Center's cross section and Molière's when $\theta < 3\times10^{-2}$ rad. Using the Dalitz screening parameter with $\mu = 1.12$, the Molière cross section is essentially recovered. However, if we use $\mu = 0.72$ for this special case, good agreement with Center's cross section is obtained for most of the range. The case shown is for 100-keV electrons in nitrogen. A similar agreement was obtained for 40-keV electrons in nitrogen. Presumably such a curve-fitting technique could be applied to other materials.

Spencer[10] has shown that if $\sigma(\theta)$ given by Eq. (6) is incorporated into the collision term of Eq. (5), the integral can be done analytically. For convenience the following substitution is made:

$$G_l = 2\pi N\int_{-1}^{+1} d\mu\;\sigma(\mu)[1 - P_l(\mu)]. \tag{9}$$

The transport mean free path λ is defined by

$$\lambda = 2/G_1; \tag{10}$$

then Eq. (5) may be written

$$\left(\frac{l}{2l-1}\right)\frac{\partial A_{l-1}}{\partial\xi} + \left(\frac{l+1}{2l+3}\right)\frac{\partial A_{l+1}}{\partial\xi} + \frac{2G_l}{G_1}A_l = 0, \tag{11}$$

where ξ is the dimensionless variable z/λ. In the limit of small-angle (Fokker-Planck)[5] collisions only,

$$2G_l/G_1 \equiv l(l+1).$$

IV. SCATTERING THROUGH A PLANE PARALLEL PLATE

Equation (11) forms an infinite set of coupled differential equations with constant coefficients. Now G_0, as defined by Eq. (9), is always zero; hence the equation for $l = 0$ is

$$\frac{1}{3}\frac{\partial A_1}{\partial\xi} = 0. \tag{12}$$

Equation (12) is simply the conservation of current.

For $l = 1$ we have

$$\frac{\partial A_0}{\partial\xi} + \frac{2}{5}\frac{\partial A_2}{\partial\xi} + 2A_1 = 0. \tag{13}$$

Truncating the series at $l = 2$, the singular solution of Bethe *et al.*[9] is recovered. However, the above truncation makes use of only the first two Legendre polynomials. The approximation is only valid if the electron distribution function is almost isotropic in μ space.

For $l > 2$, the Fourier transform of the infinite set of differential equations can be written in a matrix form

$$\vec{\vec{S}} : \vec{A} = 0, \tag{14}$$

where $\vec{A}$ is the column vector

$$\{A_2\ A_3 \ldots\ A_l\ \ldots\}$$

and $\vec{\vec{S}}$ is an infinite tridiagonal matrix.

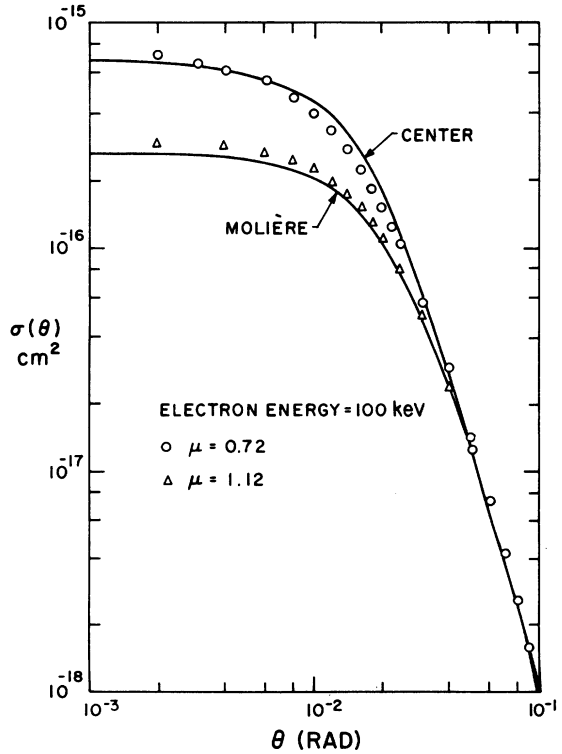

FIG. 1. Semilog plot of the elastic scattering cross section vs θ for various values of the parameter μ. Also shown are the elastic scattering cross sections used by Molière and Center.

$$\begin{bmatrix} \frac{2G_2}{G_1} & \frac{3S}{7} & 0 & 0 & \cdots & & & & & \\ \frac{3S}{5} & \frac{2G_3}{G_1} & \frac{4S}{9} & 0 & \cdots & & & & & \\ \vdots & \vdots & \vdots & \vdots & & & & & & \\ 0 & 0 & 0 & 0 & \cdots & 0 & \frac{Sl}{2l-1} & \frac{2G_l}{G_1} & \frac{S(l+1)}{2l+3} & 0 & \cdots \end{bmatrix},$$

where S is the Fourier-transform variable of the dimensionless spatial coordinate ξ. Truncating at some $l=L$, where L is odd, the homogeneous solution to the coupled set of differential equations is given by setting the determinant of $\vec{\vec{S}}$ to zero. This gives $L-1$ real roots. Hence one can write

$$A_L = \sum_{n=2}^{L} a_{L,n}\, e(S_n \xi)$$

and

$$A_{L+1} = \sum_{n=2}^{L} a_{L+1,n}\, e(S_n \xi) \equiv 0 . \tag{15}$$

Now one can go back to Eq. (11), solve for A_{L-1}, etc. in terms of A_L, or more specifically one can calculate the coefficients $a_{L-1,n}$, etc., in terms of $a_{L,n}$ from the recursion relation:

$$\left(\frac{l}{2l-1}\right) S_n a_{l-1,n} + \left(\frac{l+1}{2l+3}\right) S_n a_{l+1,n} + \frac{2G_l}{G_1} a_{l,n} = 0 . \tag{16}$$

There are $(L-1)$ unknowns $a_{L,n}$ and two unknowns, $a_{1,1}$ and $a_{0,0}$, from Eqs. (12) and (13), giving us a total of $(L+1)$ unknowns. For convenience these unknown are represented as a column vector $\vec{a}_L$. The column vector $\vec{A}$ then can be expressed as

$$\vec{A} = \vec{\vec{H}} \cdot \vec{a}_L , \tag{17}$$

where

$$\vec{\vec{H}} = \begin{bmatrix} 1 & -2\xi & h_{02}e^{S_2\xi} & \cdots & h_{0l}e^{S_l\xi} \\ 0 & 1 & 0 & \cdots & 0 \\ 0 & 0 & h_{22}e^{S_2\xi} & \cdots & h_{2l}e^{S_l\xi} \\ 0 & 0 & \cdot & \cdots & \cdot \\ \vdots & \vdots & \cdot & \cdots & \cdot \\ & & \cdot & \cdots & \cdot \\ 0 & 0 & e^{S_2\xi} & \cdots & e^{S_l\xi} \end{bmatrix} .$$

$h_{l,n}$ is obtained from the recursion relation (16) with $a_{L,n}=1 (n \geq 2)$. The column vector $\vec{a}_L$ is to be evaluated from the boundary conditions at $\xi=0$ and $\xi=t/\lambda$.

Consider an electron beam of an arbitrary but known distribution function impinging on a target of thickness t. Hence at $\xi=0$, $f(\mu \geq 0, \xi=0)$ is known, and at the far boundary $\xi=t/\lambda$, there are no particles entering the target; hence $f(\mu \leq 0, \xi=t/\lambda) \equiv 0$. Hence the boundary conditions can be written

$$\begin{aligned} f(\mu \geq 0, \xi=0) &= \sum_{n=0}^{\infty} b_{2n+1} P_{2n+1}(\mu), \\ f(\mu \leq 0, \xi=t/\lambda) &= \sum_{n=0}^{\infty} c_{2n+1} P_{2n+1}(\mu) \equiv 0 . \end{aligned} \tag{18}$$

In Eq. (18) use has been made of the fact that the odd Legendre polynomials form a complete set in the half-space. This choice is by no means unique; one could, for example, have chosen the even polynomials. However, as the current is a more readily measurable quantity than density, odd polynomials are used. Thus there are an infinite set of boundary conditions at each surface, but because of the truncation there are only $N+1$ unknowns. Hence we specify $\frac{1}{2}(N+1)$ conditions at each boundary. Making use of orthogonality, one has

$$\begin{aligned} &\int_0^1 d\mu\, P_{2n+1} f(\mu, \xi=0) = b_{2n+1}/(4n+3), \\ &\int_{-1}^0 d\mu\, P_{2n+1} f(\mu, \xi=t/\lambda) = 0 , \end{aligned} \tag{19}$$

where $n=0, \ldots, \frac{1}{2}N$.

Equations (19) are known as Marshak's boundary conditions and may be written in matrix formulation as

$$\vec{\vec{C}} : \vec{A} = \vec{B} . \tag{20}$$

The first $\frac{1}{2}(L+1)$ rows of the $\vec{\vec{C}}$ matrix are given by

$$C_{2n+1,m} = \int_0^1 d\mu P_{2n+1}(\mu) P_m(\mu),$$

$$m=0, 1, \ldots, L, \quad n=0, 1, \ldots, \tfrac{1}{2}(L+1), \tag{21}$$

and the last $\frac{1}{2}(L+1)$ rows are given by

$$C_{2n+1,m} = \int_{-1}^0 d\mu P_{2n+1}(\mu) P_m(\mu),$$

$$m=0, 1, \ldots, L, \quad n=0, 1, \ldots, \tfrac{1}{2}(L+1). \tag{22}$$

The evaluation of the integrals in (21) and (22) are given in the Appendix.

The coefficients of the column vector $\vec{B}$ are given by the right-hand sides of Eqs. (19). For the boundary conditions chosen the last $\frac{1}{2}(L+1)$ coefficients will always be zero. Substituting Eq. (17) into (20), one gets

$$\begin{aligned} &\{\vec{\vec{C}} : \vec{\vec{H}}\} : \vec{a}_L = \vec{B}, \\ &\vec{a}_L = \{\vec{\vec{C}} : \vec{\vec{H}}\}^{-1} : \vec{B}; \end{aligned} \tag{23}$$

one can solve Eq. (23) and obtain numerical values for the coefficients of the column vector $\vec{a}_L$. A solution for $\vec{A}$ is obtained, and hence a solution for the distribution function, by means of Eq. (17).

Truncating the series at some $l=L$, where L is

even, and setting the determinant of $\bar{S}$ to zero gives $L-2$ real roots. Thus there are only L unknowns and $(L+1)$ functions of A_l. Hence an additional postulate is required to determine the solution completely. So it is seen that there is a big difference as to whether one truncates at an odd- or even-order polynomial. For neutron diffusion it was shown that an even truncation resulted in an inferior approximation.[10] Because of the similarities between electron diffusion and neutron diffusion, it is expected that the even truncation is an inferior approximation.

V. ANGULAR DISTRIBUTION

The emerging electron angular distribution is given by

$$f\left(\mu, \frac{t}{\lambda}\right) = \sum_{l=0}^{N} \sum_{m=0}^{N} a_{m,l} e^{S_m \xi} P_l(\mu), \tag{24}$$

where $a_{m,l}$ are determined by means of the boundary conditions (18) and the recursion relation (16). Algebraically this involves solving an $(N+1) \times (N+1)$ matrix equation for the components of the column vector $\vec{a}_l$. These components are then substituted into the recursion relation (16) to solve for the a_{ml}. This is a laborious and time-consuming procedure for values of $N \geq 3$. For very thin targets and highly peaked distribution functions, N is a large number if the distribution function is to be accurately represented by Eq. (24). It has been found that for a distribution function having a half-width of 4° we need 50 polynomials to describe $f(\mu, \xi)$. The solution is most conveniently obtained by means of a computer.

Figure 2(a) shows a plot of the emerging distribution function of electrons. It is assumed that the electrons strike the foil normally and the distribution function is given by

$$f(\mu, 0) = \delta(\mu - 1). \tag{25}$$

The aluminum foil is assumed to be 2.5×10^{-3} cm thick. The electron energy is 919.8 keV. These assumptions result in $t/\lambda = 0.0114$. For comparison the GS (Goudsmit-Saunderson) distribution is plotted for the same conditions. The dashed curve is the single-scattering distribution, which is

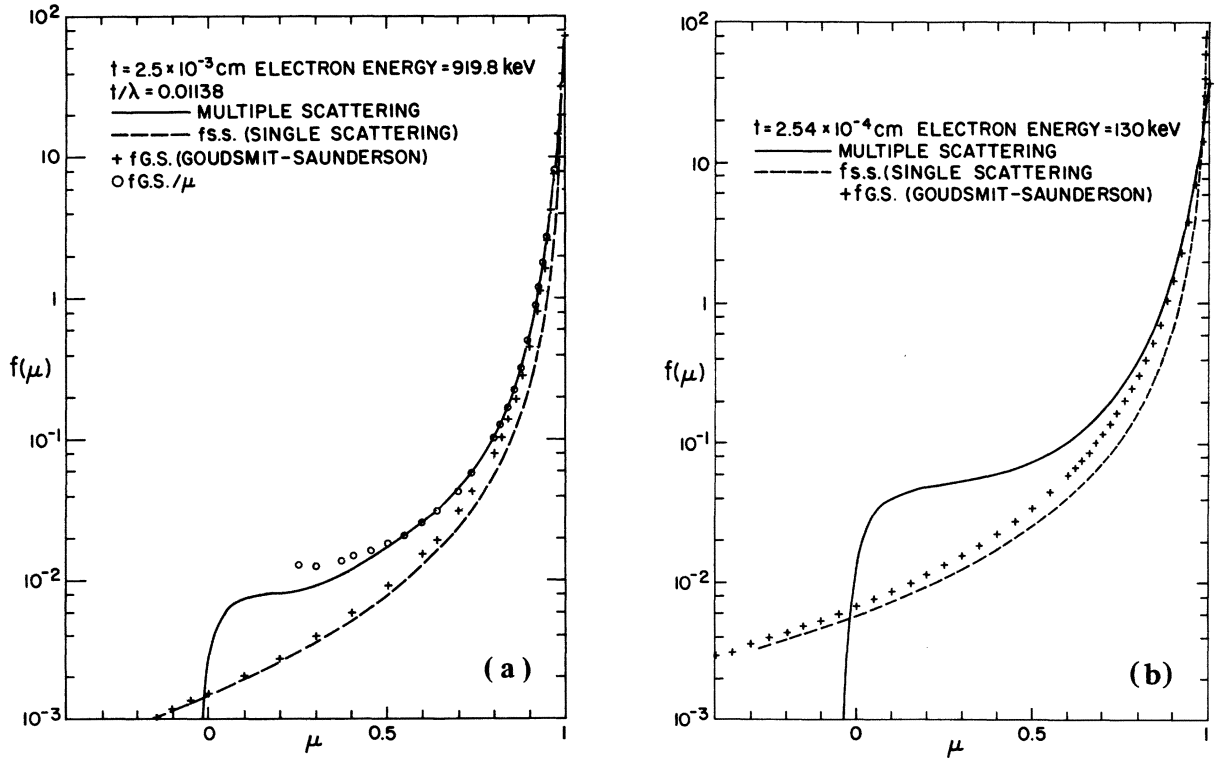

FIG. 2. (a) Emergent distribution electron function derived by the present theory (solid curve). The crosses represent the GS distribution function for identical conditions. Also shown are the single-scattering distribution (dashed curve) and the GS distribution divided by μ. As one would expect, the GS distribution emerges with the single-scattering tail; however, the present results never do. It is interesting to note that the simple correction of dividing the GS distribution by μ is in good agreement with the present theory for $\mu \leq 0.5$. The $1/e$ width of the distribution function is about 6°. (b) Same as (a), except that the effective target thickness t/λ is almost doubled. The $1/e$ width of the distribution is about 14°.

computed in the usual manner as

$$f_{ss} = 2\pi N t \sigma(\theta).$$

For small angles $0.98 \leq \mu \leq 1$, the GS distribution and the present results agree closely; however, there is a considerable divergence at larger angles. For the special case shown in Fig. 2(a) the present theory predicts that the probability of an electron scattering through an angle of 78° to be about 3 times that predicted by the GS theory. As expected, the GS distribution emerges into the single-scattering tail for large angles. Another difference between the GS distribution and the present result is that the present solution has a discontinuity at $\mu = 0$. The discontinuity is the result of the imposed boundary condition, i.e., it is assumed that at the far boundary there are no particles entering the slab. In Fig. 2(b) the chosen conditions are such that the effective target thickness, t/λ is almost double the effective target thickness for the case shown in Fig. 2(a).

It is interesting to note that for these thin targets, if one takes the GS distribution function and divides by μ,[16] the agreement between the two theories is much better, except in the vicinity of $\mu = 0$. These corrections are shown in Figs. 2(a) and 2(b). [Figure 6(a) verifies that the above correction to the GS distribution decreases the difference between the two theories in the Fokker-Planck approximation.]

There are two possible reasons for the difference at large angles between the present theory and that of Goudsmit and Saunderson: (a) the assumption that all the emerging electrons suffered the same number of collisions and (b) the boundary conditions were neglected. Let us first consider the approximation that all the electrons "see" the same target thickness. Mathematically, this is achieved by setting $\mu = 1$ on the left-hand side of Eq. (2).

Returning to the original transport equation (2) and making the Fokker-Planck expansion,[9,17] one can write

$$\mu \frac{\partial f}{\partial \xi} = \frac{\partial}{\partial \mu}(1-\mu^2)\frac{\partial f}{\partial \mu}. \tag{26}$$

Goudsmit and Saunderson, Molière, and Bethe solved Eq. (26) by setting $\mu = 1$. It is worth noting that Eq. (26) conserves current while the equation resulting from letting $\mu = 1$ conserves number density. The term they omitted by this approximation is

$$\left(\frac{1-\mu}{\mu}\right)\left(\frac{\partial}{\partial \mu}(1-\mu^2)\frac{\partial f_{GS}}{\partial \mu}\right), \tag{27}$$

where f_{GS} is the Goudsmit-Saunderson distribution. The above equation is valid if $(1-\mu) \ll 1$. Making a simple substitution

$$g = \mu f,$$

Eq. (26) becomes

$$\frac{\partial g}{\partial \xi} = \frac{\partial}{\partial \mu}(1-\mu^2)\frac{\partial (g/\mu)}{\partial \mu}$$

or

$$\frac{\partial g}{\partial \xi} = \frac{\partial}{\partial \mu}(1-\mu^2)\frac{\partial g}{\partial \mu} + \left(\frac{(1-\mu)}{\mu}\frac{\partial}{\partial \mu}(1-\mu^2)\frac{\partial g}{\partial \mu} - 2\frac{(1-\mu^2)}{\mu^2}\frac{\partial g}{\partial \mu} + \frac{2g}{\mu^3}\right). \tag{28}$$

Neglecting the terms in the large parentheses on the right-hand side of Eq. (28), the equation solved by Goudsmit and Saunderson is recovered. This approximate form of Eq. (28), however, conserves current, as does the basic transport equation. Hence on physical grounds we might expect it to be a more accurate representation than the approximate equation solved by Goudsmit and Saunderson. Hence g is just f_{GS}. For thin targets one can write

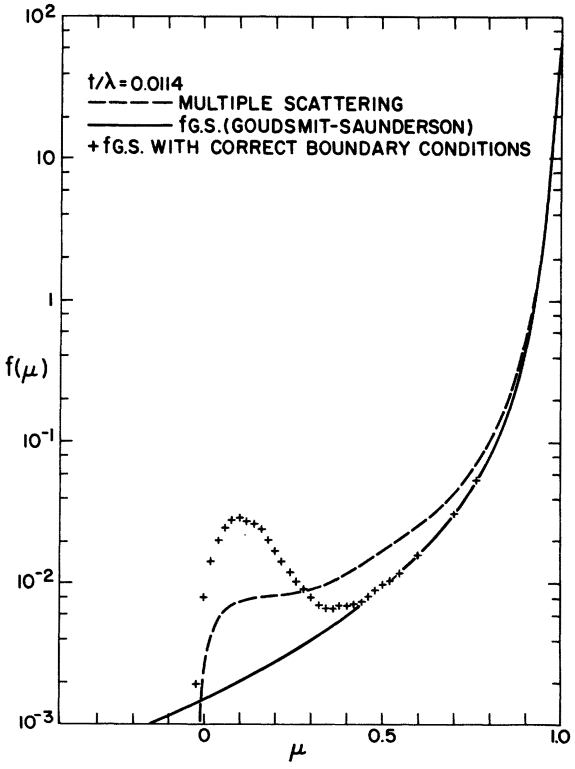

FIG. 3. Results of including the boundary conditions into the Goudsmit-Saunderson theory. The inclusion of the boundary conditions puts a bump in the GS distribution function near $\mu = 0$. For comparison the distribution function predicted by the present theory is also shown.

$$f_{GS} \approx \frac{1}{\sqrt{(2\xi)}} \exp\left(\frac{-(1-\mu)}{2\xi}\right).$$

Typically ξ, the effective target thickness, is 10^{-2}. Suppose we are interested in going out to $\mu \sim 0.85$? Then, defining a small parameter ϵ as

$$\epsilon \approx \sqrt{(2\xi)} \approx (1-\mu) \approx 0.14,$$

it is easy to show that

$$\left(\frac{1-\mu}{\mu}\right)\frac{\partial}{\partial\mu}(1-\mu^2)\frac{\partial f_{GS}}{\partial\mu} > \left\{\left(\frac{1-\mu}{\mu}\right)\frac{\partial}{\partial\mu}(1-\mu^2)\frac{\partial f_{GS}}{\partial\mu} - \frac{2(1-\mu^2)}{\mu^2}\frac{\partial f_{GS}}{\partial\mu} + \frac{2f_{GS}}{\mu^3}\right\}.$$

Hence one can conclude that f_{GS}/μ is a more accurate solution to the transport equation.

The Fokker-Planck limit is a poor approximation for thin targets, especially at large angles [see Fig. 6(a)]. In the real case the emergent distribution function will decay more slowly than that predicted by the Fokker-Planck approximation. Looking at Fig. 2(a) we see that near $\mu \approx 0.5$ the GS distribution roughly has the same slope as the single-scattering tail. Hence at these angles $f_{GS} \propto 1/(1-\mu)^2$ and it is easy to show that f_{GS}/μ is a fair approximation for angles as large as 60°. Because the GS distribution connects with the single-scattering tail for thin targets, the above approximation will be valid for the thinnest targets, provided, of course, that multiple scattering is dominant for particles that emerge in the direction of the initial beam. Wang and Guth[5] have also shown that the region of validity of the GS theory can be extended by dividing the GS distribution by μ. They obtained this result by a perturbation expansion about the GS distribution.

The above correction does not include the fact that the Goudsmit-Saunderson result neglects the boundary condition. To determine the effect of the boundary conditions, the transport equation (2) was solved by letting $\mu = 1$ (which makes the actual path length traveled by the electron the independent variable) and the results of the calculation are shown in Fig. 3. Once again t/λ was chosen to be 0.0114 and the initial electron energy to be 919.8 keV. The inclusion of the boundary condition has a large effect between $0 < \mu < 0.4$. However, for $\mu > 0.4$, the difference between including the boundary conditions and omitting them is negligible. So it appears that the boundary conditions become important near $\mu \approx 0$, whereas the difference between the present and earlier theories for $\mu < 0.5$ is because of the assumption that all electrons suffered the same number of collisions.

Spencer and Blanchard[12] have calculated the emerging electron distribution function from a gold foil for the experimental conditions of Hanson, Lanzl, Lyman, and Scott.[11] They have used the relevant single-scattering cross section that included both relativistic effects and deflections due to inelastic scattering by orbital electrons. The agreement between experiment and theory is good for angles $\leq 10°$. However, at larger angles there is a discrepancy of 15%, which is greater than the expected experimental error. The $1/e$ width of the emergent electron distribution is about 2°, and even 50 polynomials inadequately represent the distribution function. Instead, the results of Spencer and Blanchard[18] (which is the Goudsmit-Saunderson distribution function) were divided by $\cos\theta$. Figure 4 shows the original Spencer-Blanchard theory, the present correction, and the experimental points of Hanson, Lanzl, Lyman, and Scott. Although the corrected theory is not perfect, it is clearly in better agreement with the experimental results. Hence it is clear that the GS theory (and Molière's) is good only for small angles. At large angles the usual assumption that the electron distribution function is just the single-scattering tail is incorrect.

For thicker targets, the GS theory breaks down completely as one would expect. Figure 5 shows

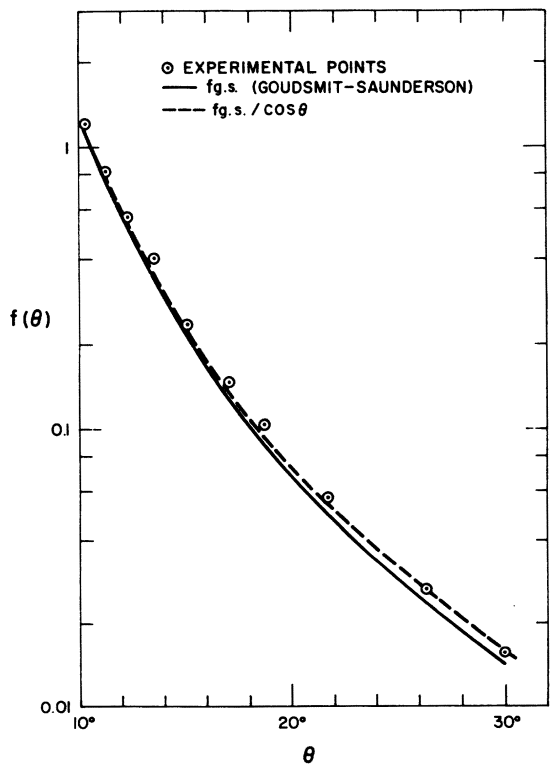

FIG. 4. Comparison of the experimental data of Hanson, Lanzl, Lyman, and Scott, the GS distribution as derived by Spencer and Blanchard (solid curve) and the corrected GS distribution function (dashed curve).

a comparison of the present results with Goudsmit and Saunderson's theory for $t/\lambda = 0.262$. When $t/\lambda > 0.2$, Bethe, Rose, and Smith[9] have pointed out that the first two polynomials adequately represent the distribution function. Figure 5 also shows the results of truncating the series at the 5th, 9th, and 17th polynomial. Except for the region near $\mu \approx 0$, all three representations agree very closely. The reason for the poor agreement at $\mu \approx 0$ is that the boundary conditions impose a discontinuity at $\mu = 0$. We would require an infinite number of polynomials to represent such a discontinuity.

Finally, in Figs. 6(a) and 6(b) a comparison is made between the small-angle approximation, which a number of authors[1-4, 9] have used with the complete collision integral. When $t/\lambda = 0.026$ there is a considerable discrepancy throughout the range. In Fig. 6(b) t/λ is increased by a factor of 10, and Fokker-Planck approximation is in better agreement with the distribution function evaluated for the complete collision integral.

VI. NUMBER DENSITY OF ELECTRONS ACROSS SLAB

The electron number density is defined as

$$N = \int_{-1}^{+1} d\mu f(\mu, z) \tag{29}$$

or, for our special case,

$$N = 2A_0(z), \tag{30}$$

the coefficient of the zeroth-order Legendre polynomial.

Figure 7 shows the variation of A_0 across a slab of aluminum. In this case $t/\lambda = 0.262$. The solid line is the result of assuming a δ-function distribution for the electrons striking the target. The crosses are for a distribution $f(\mu, 0) = 50e^{-25\theta^2}$. This corresponds to a $1/e$ width of $\frac{1}{5}$ rad. In both cases only 18 polynomials have been used.

In the case of the δ-function input, there is a

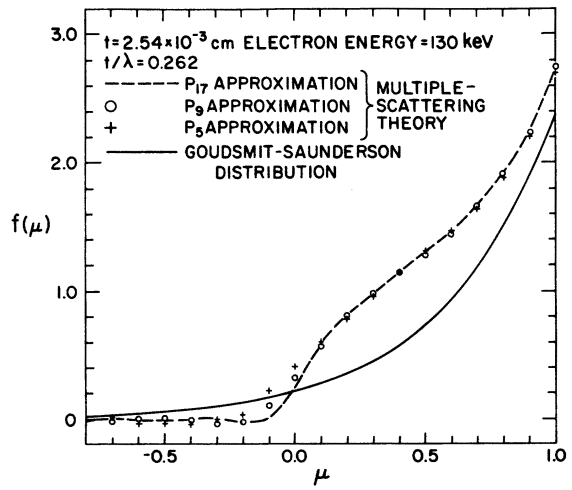

FIG. 5. Plots of the emergent electron distribution function for a relatively thick target, as predicted by the present theory (dashed curve) and Goudsmit and Saunderson's theory. Also shown are predictions of present theory using 10 polynomials (P_9 approximation) and 6 polynomials (P_5 approximation).

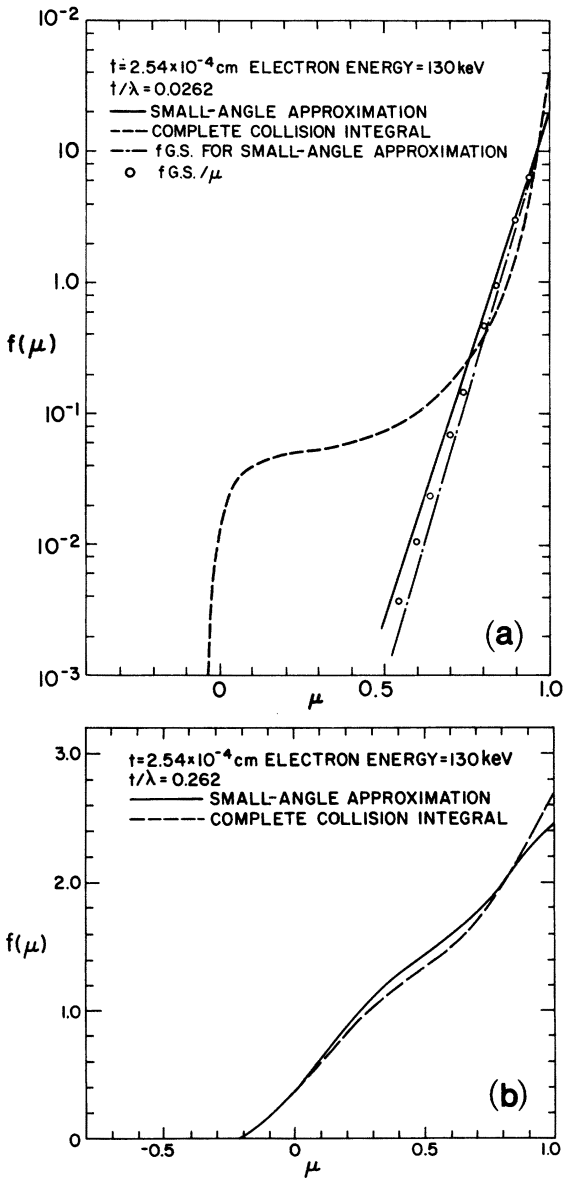

FIG. 6. (a) Effect of the Fokker-Planck approximation for thin targets and highly peaked distribution functions. Once again the GS distribution decays more rapidly than the distribution predicted by the present theory. Also shown is the correction to the GS distribution. (b) Same as (a), except that the effective target thickness is increased by a factor of 10.

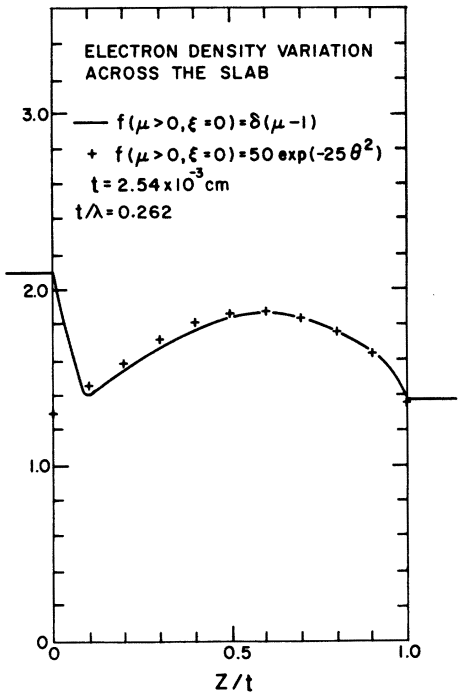

FIG. 7. Plot of the number density variation across the slab for an effective target thickness of $t/\lambda = 0.262$. The solid curve is for a δ function impinging on the aluminum foil; the crosses are for an incident distribution function with a 10° spread.

narrow region near $\xi = 0$ where there are convergence problems, i.e., 18 polynomials are insufficient to represent a δ function. However, as the electron beam traverses the target it spreads and the 18 polynomials are better able to represent the electron distribution function. For the case of the initial distribution function having a width of about 10°, the 18 polynomials are an adequate representation through the complete slab. Thus it is seen that if one starts with a δ function of electrons, there will always be a region in space where the finite number of polynomials cannot represent the distribution function. This is a limitation of the present computational method of approach. However, for the case chosen it turns out that the emergent electron-beam spread is so much greater than 10° that the error introduced by replacing a δ function with a function of width $\frac{1}{5}$ rad is less than 5% through the whole slab.

The reason the number density initially increases is because the electron beam is diffusing in velocity space, and if current is to be conserved the density has to increase. The decrease in the number density of $z/t > 0.6$ is because at this point the beam is so spread out that backscatter dominates and hence the electron density decreases. It turns out that the Bethe, Rose, and Smith[9] criteria for separating thick and thin targets is the approximate point where backscatter begins to dominate. Physically this says that a target is thin if backscatter is unimportant.

VII. CONCLUSIONS

The electron transport equation has been solved exactly for diffusion through a plane parallel plate. The only assumption made is that the energy is constant. Hence we expect the results to be good for thin targets, i.e., targets much thinner than the Bethe range[10] for energy loss. Contrary to general belief and predictions of earlier theories[1-4] the emergent electron distribution function does not coincide with the single-scattering one even for the thinnest target considered ($t/\lambda = 0.0114$). For thick targets ($t/\lambda > 0.2$) earlier theories are a poor approximation for all angles. The incorporation of energy loss because of inelastic excitation and ionization can be included in a straightforward manner. The calculation will hopefully be completed shortly.

ACKNOWLEDGMENTS

The author is greatly indebted to Dr. J. D. Daugherty for his suggestion of using the spherical-harmonic expansion. Enlightening discussions with Dr. E. R. Pugh are also acknowledged. P. J. Pfeiffer's help with the numerical computation is greatly appreciated.

APPENDIX: ORTHOGONALITY RELATIONS FOR HALF-SPACE

Consider the differential equation for Legendre polynomials,

$$\frac{d}{d\mu}(1-\mu^2)\frac{dP_\alpha}{d\mu} + \alpha(\alpha+1)P_\alpha = 0 . \tag{A1}$$

Multiplying (A1) by $P_\beta(\mu)$ and integrating over the half-space, one gets

$$\int_0^1 d\mu P_\beta(\mu)\left(\frac{d}{d\mu}(1-\mu^2)\frac{dP_\alpha}{d\mu} + \alpha(\alpha+1)P_\alpha\right) = 0 .$$

Integrating the above equation by parts results in

$$\int_0^1 d\mu \left((\mu^2-1)\frac{dP_\beta}{d\mu}\frac{dP_\alpha}{d\mu} + \alpha(\alpha+1)P_\alpha(\mu)P_\beta(\mu)\right)$$

$$= P_\beta(0)\frac{dP_\alpha}{d\mu}\bigg|_{\mu=0} . \tag{A2}$$

Interchanging α and β in (A2) and subtracting (A2) from the resulting equation gives

$$[\beta(\beta+1)-\alpha(\alpha+1)]I_{\alpha,\beta} = P_\alpha(0)\frac{dP_\beta}{d\mu}\bigg|_{\mu=0} - P_\beta(0)\frac{dP}{d\mu}P_\alpha\bigg|_{\mu=0}, \quad \text{(A3)}$$

where

$$I_{\alpha,\beta} = \int_0^1 d\mu\, P_\alpha P_\beta .$$

Let $\alpha = 2m$ and $\beta = 2n+1$, where m and n are integers. The second term on the right-hand side of (A3) is zero. Making use of the recurrence relation

$$\frac{d}{d\mu}P_{2n+1} = \frac{1}{\mu^2-1}[(2n+1)\mu P_{2n+1} - (2n+1)P_{2n}],$$

Eq. (A3) reduces to

$$[(2n+1)(2n+2) - 2m(2m+1)]I_{2m,2n+1} = (2n+1)P_{2m}(0)P_{2n}(0) \quad \text{(A4)}$$

or

$$I_{2m,2n+1} = \frac{(-1)^{n+m}(2n+1)[1\cdot 3\cdot 5\cdot\cdots(2n-1)][1\cdot 3\cdot 5\cdot\cdots(2m-1)]}{[(2n+1)(2n+2)-2m(2m+1)][2^{m+n}(n!)(m!)]} . \quad \text{(A5)}$$

When $\alpha = 2m+1$ and $\beta = 2n+1$, it is clear that

$$I_{2m+1,2n+1} = \delta_{m,n}\frac{1}{4n+3} . \quad \text{(A6)}$$

Finally, it is known that

$$\int_{-1}^{+1} P_{2m}P_{2n+1}\,d\mu = 0;$$

hence

$$\int_{-1}^{0} P_{2m}P_{2n+1}\,d\mu = -I_{2m,2n+1} . \quad \text{(A7)}$$

*Work supported by Advanced Research Projects Agency, monitored by the Office of Naval Research, Alexandria, Va., under Contract No. N00014-70-C-0427.

[1]E. J. Williams, Proc. R. Soc. Lond. **169,** 531 (1939); see also Phys. Rev. **58,** 292 (1940).
[2]S. Goudsmit and J. L. Saunderson, Phys. Rev. **57,** 24 (1940).
[3]G. Molière, Z. Naturforsch. **3a,** 78 (1948).
[4]H. A. Bethe, Phys. Rev. **89,** 1256 (1953).
[5]Ming Chen Wang and Eugene Guth, Phys. Rev. **84,** 1092 (1951).
[6]E. Breitenberger, Proc. R. Soc. Lond. **250,** 514 (1959).
[7]B. Davison, *Neutron Transport Theory* (Oxford U. P., Oxford, England, 1957), pp. 116–137.
[8]K. M. Case and P. F. Zweifel, *Linear Transport Theory* (Addison-Wesley, Reading, Mass., 1967), pp. 194–214.
[9]H. A. Bethe, M. E. Rose, and L. P. Smith, Proc. Am. Philos. Soc. **89,** 1256 (1938).
[10]L. V. Spencer, Phys. Rev. **98,** 1587 (1955).
[11]A. O. Hanson, L. M. Lanzl, E. M. Lyman, and M. B. Scott, Phys. Rev. **84,** 634 (1951).
[12]L. V. Spencer and C. H. Blanchard, Phys. Rev. **93,** 114 (1954).
[13]B. P. Nigam, M. K. Sundarsen, and Ta-You Wu, Phys. Rev. **115,** 491 (1959).
[14]J. W. Motz, Haakon Olsen, and H. W. Koch, Rev. Mod. Phys. **36,** 881 (1964).
[15]R. E. Center, Phys. Fluids **13,** 79 (1970).
[16]This simple correction of the Goudsmit-Saunderson (GS) distribution was suggested by Dr. R. D. Sharma.
[17]For thin targets and initial δ-function distribution the Fokker-Planck expansion is a poor approximation because both f and σ are sharply peaked functions in the collision integral. However, the Fokker-Planck expansion is used to justify the correction by dividing the GS distribution by μ.
[18]The author is greatly indebted to Dr. L. V. Spencer for sending the original plots of the calculated distribution function.